Nano Select

RESEARCH ARTICLE OPEN ACCESS

Hydrogen Evolution via Oxygen Tolerant [NiFe]-Hydrogenase Immobilized on TiO_2 Nanotubes

Hwapyong Kim[1] | Ki Nam Kim[1] | Sung Hyun Lee[1] | Chang-Hoon Nam[2] | Young-Sam Lee[2] | Su-Il In[1]

[1]Department of Energy Science & Engineering, Daegu Gyeongbuk Institute of Science and Technology (DGIST), Daegu, Republic of Korea | [2]Department of New Biology, Daegu Gyeongbuk Institute of Science and Technology (DGIST), Daegu, Republic of Korea

Correspondence: Young-Sam Lee (lee.youngsam@dgist.ac.kr) | Su-Il In (insuil@dgist.ac.kr)

Received: 9 June 2025 | **Revised:** 1 September 2025 | **Accepted:** 10 September 2025

Funding: This study was funded by the Ministry of Science and ICT in Korea (2021R1A2C2009459 and 1.250022).

Keywords: aerobic condition | electropolymerization | hydrogenase | hydrogen evolution reaction | TiO_2 nanotube

ABSTRACT

[FeFe]-hydrogenase has been of great interest due to its high enzymatic activity for hydrogen evolution reactions (HERs). However, the big challenge of [FeFe]-hydrogenase is a significant performance degradation in aerobic conditions. On the other hand, [NiFe]-hydrogenase of *E. coli* has an oxygen tolerant property. Therefore, using [NiFe]-hydrogenase is an effective solution to avoid performance degradation in aerobic conditions. Herein, we extracted [NiFe]-hydrogenases from *E. coli* and immobilized them on the TiO_2 nanotube (TNT) electrode prepared by pyrrole-based electropolymerization for application in aerobic conditions. As a result, we can confirm that [NiFe]-hydrogenases coated TNT electrode demonstrates the increased HER activity underaerobic condition than control samples in in-vitro activity test using methylene viologen and linear sweep voltammetry.

1 | Introduction

Nowadays, hydrogen is a future energy source becuase it is carbon-neutral. Hydrogen has a high energy density and emits only water as a result of combustion. However, most hydrogen is produced from fossil fuels with steam methane reforming that emits CO_2 during the chemical reaction. To produce hydrogen without CO_2 emission, electrochemical water splitting [1], photoelectrochemical cells (PEC) [2–7], photocatalysis [8, 9], and a bioelectrochemical system (BES) are typical options for clean hydrogen production techniques. Among them, BES is promising clean hydrogen production technology because it utilizes biomass or waste as feedstock and can operate under mild conditions with lower energy demand. For example, a microbial electrolysis cell (MEC) is a technology using a microbial anode to degrade the organic matter and supply protons to the cathode to produce hydrogen [10]. MEC can also convert to a microbial fuel cell (MFC) to degrade organic matter and produce electricity when electricity is not supplied for MEC operation [11–13]. However, most of the BES use noble metals for cathode catalysts. These catalysts have many limitations for commercialization, such as high cost, resource depletion, and unbalanced reserves by location. To solve these problems in BES, cathodic nanomaterials should be replaced with catalysts that are inexpensive and not limited by resource depletion.

Hydrogenase is the metalloenzyme that catalyzes the reduction and oxidation of hydrogen reversibly, and its catalytic activity (10^4 s^{-1}) is high enough to be comparable with Pt catalyst [14–16]. The major hydrogenases are classified as [FeFe]-hydrogenases and [NiFe]-hydrogenases [17]. [FeFe]-hydrogenase has a higher hydrogen evolution rate and is highly sensitive to oxygen and active under strictly anaerobic conditions [18, 19]. Because of this stringent requirement of anaerobic conditions, studies of [FeFe]-hydrogenases are operated in the glove box. It is difficult to utilize as electrolysis cells in the aerobic condition. On the

other hand, [NiFe]-hydrogenase displays better stability than [FeFe]-hydrogenases [18, 20, 21]. Various microorganism strains are studied as the source of hydrogenases: microalgae [18, 19], anaerobes [22–32], cyanobacteria [33–38], *Escherichia coli (E. coli)* [39–43], etc. [44]. Because of it's high catalytic activity for hydrogen conversion [14–16], hydrogenases has got attention in recent studies for eco-friendly hydrogen production in both in vivo [22–28, 33–36, 39–43, 45–48] and in-vitro condition [29–32, 37, 38, 44]. Most in-vitro hydrogenase-based hydrogen production studies were performed by manufacturing electrodes with attached hydrogenase. Both physisorption [31, 32] and covalent bonding [50] can attach hydrogenase to the electrode surface. Among them, the hydrogenase electrode made by adsorption shows better performance [27]. Attaching hydrogenase to the electrode surface by physisorption has a disadvantage that physiosorbed hydrogenase can be left from the electrode surface over time because of weak bond strength. Polypyrrole (PPy) membrane fabricated by electropolymerization can be a solution to immobilize physiosorbed hydrogenase [28]. Surface properties of the electrode are also crucial because they relate to the interaction between the hydrogenase active site and electrode surface: an electrode with a sharp nanoporous surface diameter has higher hydrogen evolution than the electrode with a smooth and larger diameter nanopore [31]. Some hydrogenase electrodes are operated with external bias application [15, 30, 37], but many studies combine hydrogenase with photosystem and photocatalyst to replace bias or improve production rate by photocurrent [29, 31, 32, 38, 44, 49–51]. Some recent studies have chosen a biomimetic strategy to synthesize novel catalytic nanostructures by using the mechanism of the hydrogenase active site cofactor [52, 53]. Hydrogenase 1 of *E. coli* is an oxygen-tolerant membrane-bound [NiFe]-hydrogenase. It has lots of benefits of using *E. coli*, such as low cost and low depletion impact. Therefore, hydrogenase 1 is a good candidate for hydrogen-producing nanomaterials of BES. Its gene is made up of six gene operons, hyaABCDEF, and the first two genes, hyaA (40.6 kDa) and hyaB (66.2 kDa), encode the small and large subunits of hydrogenase 1, which are core subunits that catalyze both hydrogen oxidation and proton reduction reaction [15]. Hydrogenase 1 is a heterodimer containing hyaA and hyaB. In *E. coli*, hydrogenase 1 builds a complex with cytochrome b, the transmembrane protein part of the electron transport chain. This complex is fixed on the periplasmic side of the cytoplasmic membrane by the C-terminal α helix transmembrane motif of hyaA and cytochrome b. Electron is transferred from the heme group of cytochrome b to two [Fe_4S_4] clusters of hydrogenase 1, and the reversible reaction of hydrogen oxidation and proton reduction occurs on the [Fe_4S_4] cluster. Comparing most hydrogenases, hydrogenase 1 has a significant advantage: relatively strong oxygen tolerance. Also, previous studies have demonstrated hydrogen proudction with hydrogenase 1 both in-vivo and in-vitro [47, 48].

2 | Experimental Section/Methods

2.1 | Hydrogenase 1 Gene Transformation to *E. coli* Strain BL21 (DE3)

For the overexpression of the hydrogenase 1 gene, BL21(DE3) was utilized as the host cell for our recombinant plasmid vectors. *E. coli* BL21 strains are deficient in Lon protease, soluble in the cytoplasm, and OmpT protease, located on the outer membrane. Because of the absence of two proteases, the overexpressed proteins of BL21 are less degraded, so BL21 is preferred for recombinant protein expression. BL21(DE3) has λDE3 lysogen, which expresses T7 RNA polymerase by lacUV5 promoter, while other BL21 strains do not have it. Because transcription of the inserted gene in the pET-28b(+) plasmid vector is promoted by the T7 promoter; therefore, BL21(DE3) was selected. The expression of lacUV5 promoter is related to lac repressor and can be induced by IPTG, isopropyl β-D-1-thiogalactopyranoside, a molecular mimic of allolactose but does not hydrolyze by β-galactosidase. As a result, the expression of an inserted gene could be induced by a small amount of ITPG addition in the medium. The protocol of gene transformation for BL21(DE3) is similar but slightly different from that for TOP10. BL21(DE3) competent cell was melted on ice for 10 min, added 1 μL of a recombinant plasmid vector, mixed smoothly by tapping, and incubated on ice for 30 min. Heat shock was applied to the cell at 42°C for 20 s and placed it on ice for 2 min. LB medium of 500 μL was added and incubated at 37°C at 200 rpm for 1 h. Then, it was centrifuged at 13,000 rpm for 1 min, abandoned 450 μL of supernatant, and eluted it for resuspension. Only recombinant cell AB was spread on an agar plate with kanamycin (50 μg mL^{-1}), and the other four recombinant cells were spread on an agar plate with both kanamycin (50 μg mL^{-1}) and ampicillin (50 μg mL^{-1}). Agar plates were incubated at 37°C overnight and checked the colony appearance.

2.2 | Enzyme Electrode Fabrication by Electropolymerization

To fabricate the hydrogenase immobilized electrode, a TiO_2 nanotube (TNT) was first prepared by electrochemical anodization of Ti foil. The hydrogenase was then deposited onto the surface of the TNT, followed by electropolymerization to form a polypyrrole for hydrogenase immobilization. Prior to anodization, the Ti foil was cleaned by sonication in acetone, ethanol, and deionized water for 10 minutes each. The two-electrode electrochemical cell was set to perform the electrochemical anodization, in which Ti foil works as the working electrode and carbon paper works as a counter electrode, and both electrodes were kept apart at 2 cm. The electrolyte for Ti foil anodization was ethylene glycol with 0.5 wt.% NH_4F and 2.0 vol.% DI water. 40 V was applied for 30 min to perform anodization as reported previously [11, 12]. After anodization, the anodized Ti foil surface was washed with DI water to wash out the electrolyte, sonicated in ethanol for 2 min to clean contaminants and debris, and annealed at 450°C for 2 h. The TNT array was cut into a circular form with a diameter of 3.0 cm (7.0 cm^2 area). Hydrogenase buffer (0.284 and 0.218 mg mL^{-1}) was prepared for the hydrogenase electrode by mixing 1 mL of hydrogenase 1 sample by Ni affinity purification and 9 mL of Tris-HCl buffer (pH 8.0). The TNT array was immersed in 10 mL of enzyme buffer for 12 h to deposit the enzyme on the TNT array surface. Then, we composed a three-electrode electrochemical cell to perform the electropolymerization, in which the enzyme-deposited TNT array works as a working electrode, Ag/AgCl reference electrode (3.0 M KCl, EC-frontier, Japan) works as a reference electrode. Pt wire works as a counter electrode, and both

electrodes were kept apart at a distance of 2 cm. The electrolyte for electropolymerization was 0.1 M KCl with 2 mM pyrrole by mixing 7.455 g of KCl, 139 µL of pyrrole, and 1 L of DI water. We applied 0.7 V for 20 min. Finally, the electropolymerized electrode was submerged in 10 mL of Tris-HCl buffer (pH 8.0) and stored at 4°C.

2.3 | Electrochemical Analysis for Hydrogenase Electrode

LSV measurement of enzyme electrodes was performed to verify the enzyme's activity. Potentiostat (Bio-Logic, VSP model, France) was set in cyclic voltammetry mode with three electrode configurations. The working electrode was connected to the enzyme electrode, the reference electrode was connected to the Ag/AgCl reference electrode, and the counter electrode was connected to the Pt wire. Each electrode was spaced about 2 cm. To prepare electrolytes for the hydrogenase electrode, we made 60 mM MES buffer (60 mM MES monohydrate, 60 mM HEPES, 60 mM TAPS, and 0.1 M NaCl). The voltage range was from +0.0 to −1.0 V_{RHE} with a scan rate of 5 mV s^{-1} in aerobic conditions. Tafel plots were converted from *J*–*V* plots. Electrochemical impedance spectroscopy (EIS) was measured by applying 0.25 V_{RHE} within 100 kHz–50 mHz. Chronoamperometry was measured by applying 0.25 V_{RHE}. The electrochemical active surface area (ECSA) was measured at the region of non-Faradaic potential range with 5–100 mV s^{-1} scan rates.

3 | Results

3.1 | Verifying of Hydrogenase Gene and Protein Expression

3.1.1 | Agarose Gel Electrophoresis Result of Hydrogenase 1 and Western Blot Analysis of Recombinant *E. coli* With IPTG

Correct recombinant plasmid vectors were achieved through repeated construction. The agarose gel electrophoresis result of the hydrogenase 1 recombinant plasmid vectors was linearized by a restriction enzyme (Figure 1a). hyaAB had about 5 and 3 kb bands. Therefore, the correct size of each vector and gene should be pET-28b ≈ 5.3 kb, hyaAB ≈ 2.9 kb; these correspond with the result of agarose gel electrophoresis. DNA sequencing results also showed that only small number of silent mutations do not affect expressed proteins. The western blot was conducted to check recombinant *E. coli* with the hydrogenase 1 gene (Figure 1b). It was identified that all recombinant *E. coli* strains produce the hydrogenase 1 subunit from the western blot. Wild-type *E. coli* did not show any significant bands, proving that every wild-type protein of *E. coli* cannot form specific binding with the His-probe antibody (H-3). However, all strains showed a thick band correlated with hyaA, the small subunit of hydrogenase 1. Most features correspond with the design of recombinant plasmid vectors. Also, the size of the hydrogenase of recombinant *E. coli* was measured by SDS-PAGE (Figure S1).

3.1.2 | SDS-PAGE Analysis of Ni Affinity Purification Fractions depending on Detergent Treatment

The results of nickel affinity chromatography were analyzed by SDS-PAGE (Figure 2). In most experiments, we could observe the bands that correspond with subunits of hydrogenase 1. By comparing detergent addition, hyaA expression without detergent (Figure 2a, b) was weaker thanwith detergent (Figure 2c, d). Addition of Triton X-100, a nonionic detergent, dissolved the lipid bilayer of the cytoplasmic membrane, which results in increased solubility of hyaA because the hyaA subunit has a C-terminal α helix transmembrane motif, which works as an anchor.

We measured the absorbance of the Bradford reagent and sample mixture at 595 nm using a spectrophotometer for the Bradford protein assay. The standard curve of albumin is shown in Figure S2. As a result, we got the trend line equation of the standard curve, $y = 0.19905 \ln(x + 0.06493) + 0.50374$, and calculated the concentration of purified protein samples as 0.452 mg mL^{-1} for the purified sample obtained (Figure S2).

3.2 | Evaluation of Hydrogen Evolution of Hydrogenase

3.2.1 | Hydrogenase In-vitro Activity Assay

In the in-vitro test, we used methylene viologen, a redox-sensitive dye that is blue in reduced form and colorless in oxidized form as an electron donor for hydrogenase 1 to hydrogen production [54, 55] and sodium dithionite as a reducing agent to reduce methylene viologen (Figure 3a). Sodium dithionite reduces oxidized methylene viologen ($S_2O_4^{2-} \rightleftharpoons 2SO_2^-$; $MV^+ + SO_2^{2-} \rightarrow MV^0 + SO_2^-$), then the electron of reduced methylene viologen transfers to hydrogenase [56, 57]. Hydrogen was quantified over time by gas chromatography (Figure 3b). After 2 h in-vitro test, 0.224 µmol was evolved in the vial.

3.2.2 | Hydrogenase In-Vitro Activity Assay

To investigate the electrochemical hydrogen evolution reaction (HER) performance of the hyaAB extracted from *E. coli*, the resulted hyaAB enzyme was immobilized on the bare TNT electrode, then polypyrrole (PPy) was electropolymerized (labeled as TNT/hyaAB/PPy) used as working electrode. To confirm the reproducibility of the electrode performance, we measured LSV across multiple batches (Figure S3). An average cathodic current density of 0.205 mA cm^{-2} was observed at an applied 0.25 V_{RHE}. The TNT/hyaAB/PPy cathode exhibited a reduction peak from −0.25 V_{RHE}, which was the same as the previous study, which reported the reduction peak of the electropolymerized hydrogenase electrode is −0.25 V_{RHE} [50], and the hydrogenase electrode showed an improved reduction current than the TNT cathode without enzyme as the potential drops below the reduction peak. Under anaerobic conditions, LSV plots showed no significant changes with the presence of oxygen (Figure 4a). To evaluate the interfacial reaction kinetics using [NiFe]-hydrogenase (hyaAB), charge carrier resistances were determined by Nyquist plot analysis (Figure 4b). In Figure 4b, an equivalent circuit is inserted, and this circuit includes electrolyte solution resistance

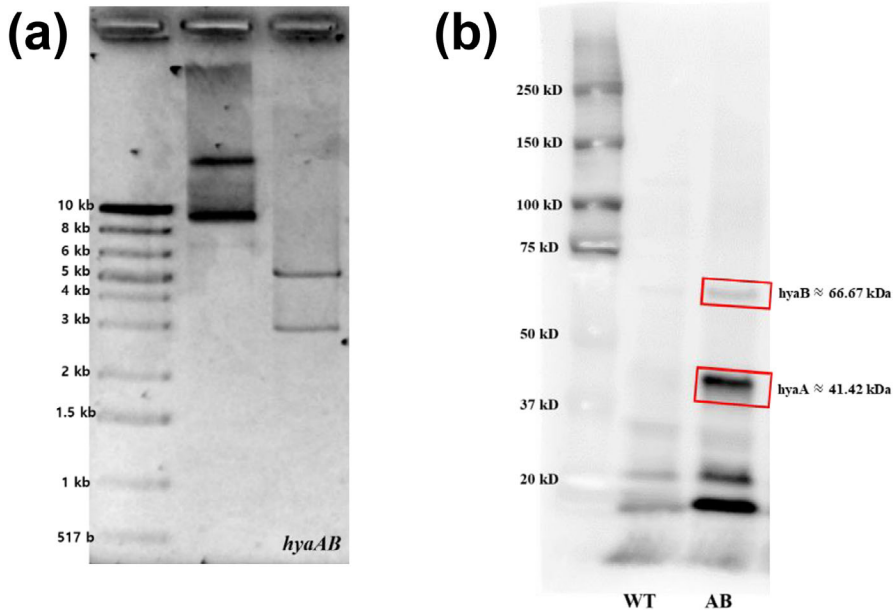

FIGURE 1 | (a) Agarose gel electrophoresis analysis of recombinant plasmid vectors treated with a restriction enzyme. (b) Western blot analysis of recombinant *E. coli* treated with IPTG.

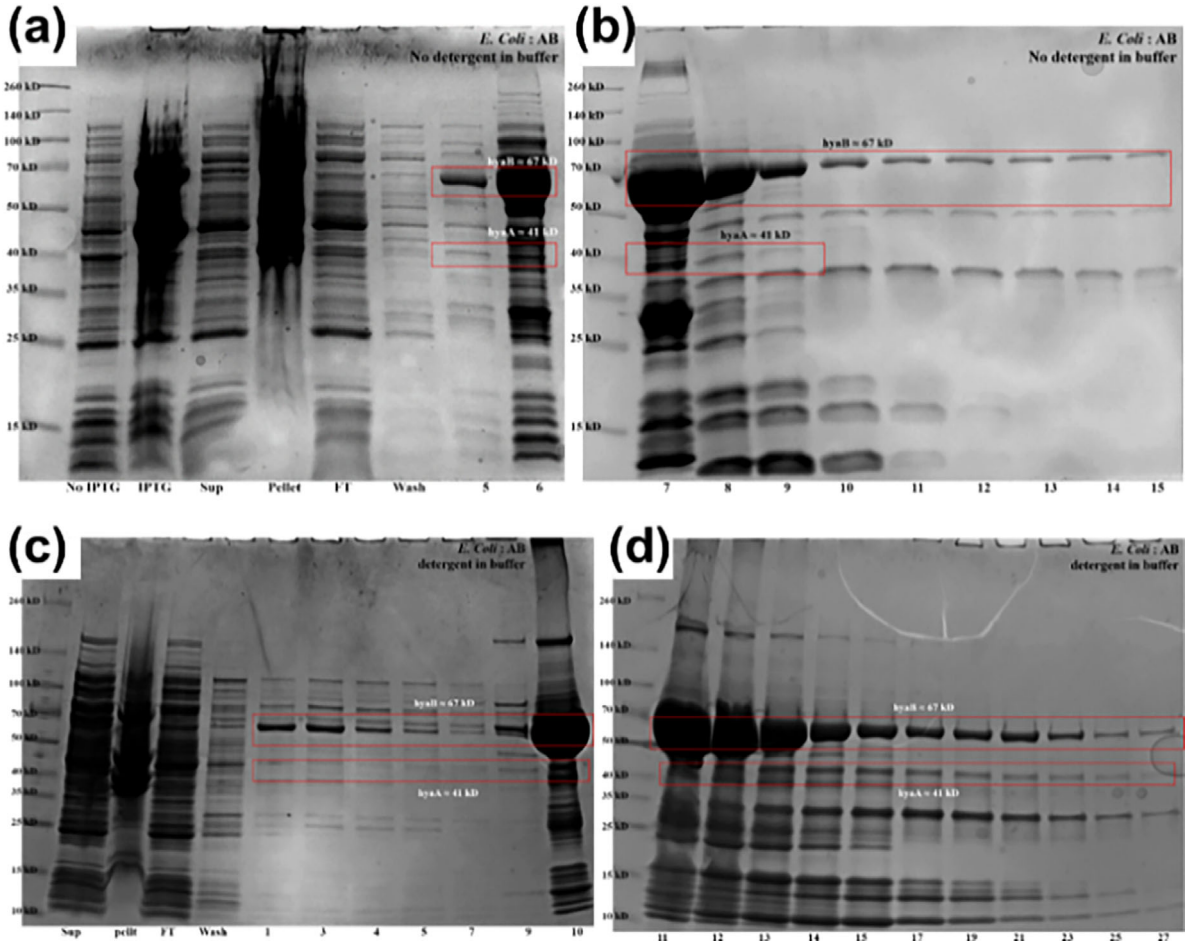

FIGURE 2 | SDS-PAGE analysis of Ni affinity purification products of (a) No IPTG, IPTG, Sup, Pellet, FT, Wash, from 5th to 6th eluted samples without detergent, (b) from 7th to 15th eluted samples without detergent, (c) No IPTG, IPTG, Sup, Pellet, FT, Wash, from 5th to 6th eluted samples with detergent, and (d) from 7th to 15th eluted samples with detergent. FT = supernatant which flows through Ni column; IPTG = cell treated with IPTG; No IPTG = cell not treated with IPTG; numbers = order of eluted sample; Pellet = pellet of cell lysate; Sup = supernatant of cell lysate; Wash = wash buffer which flows through Ni column before eluting buffer.

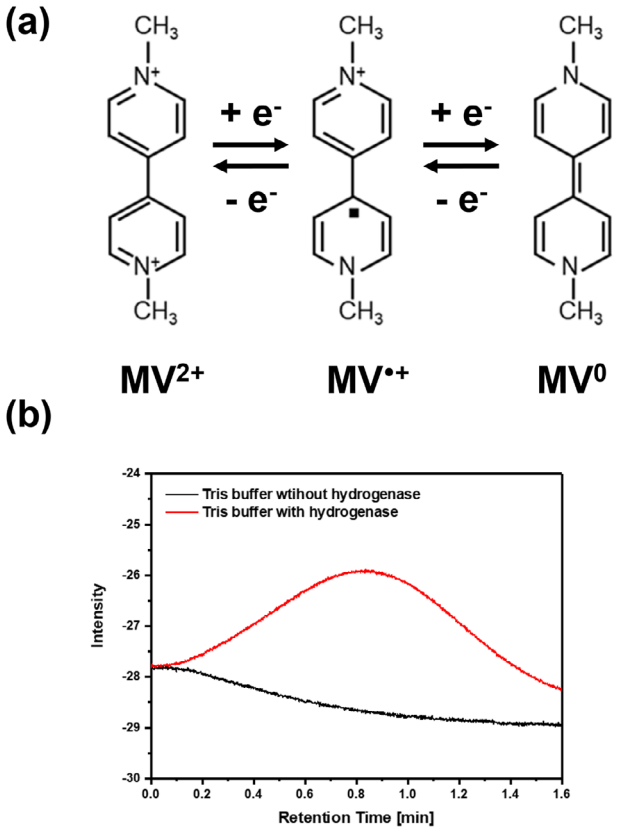

FIGURE 3 | (a) Schematic illustration of methylene viologen redox transformations and (b) gas chromatography results in detecting hydrogen from in-vitro test after 2 h later of hydrogenase addition.

(R_s), charge transfer resistance (R_{ct}), and constant phase element (CPE), where a smaller charge transfer resistance indicates the faster charge transfer kinetics of interfacial electrochemical reaction [58]. The Nyquist plots exhibited that the R_{ct} value of TNT/hyaAB/PPy was smaller than that of bare TNT, indicating faster charge transfer by [NiFe]-hydrogenase on the TNT electrode. Also, a chronoamperometry test was conducted to evaluate the stability of TNT/hyaAB/PPy. The initial current density value was measured as 0.124 mA cm^{-2}. After 3 h operation, the current density decreased to be 0.081 mA cm^{-2} with 65.32% current density retention (Figure 4c).

To evaluate the pH on the enzyme immobilized electrode, we conducted LSV plots, Tafel plots, and ECSA analysis under different pH conditions of MES buffer (Figure 5). In their LSV plots, the cathodic current density of TNT/hyaAB/PPy exhibited the following order of pH = 10.5 (9.65 mA cm^{-2}), pH = 7.5 (5.80 mA cm^{-2}), and pH 4.5 (4.08 mA cm^{-2}) applied at 1.0 V_{RHE} (Figure 5a). These results denote that the overall electrocatalytic hydrogen evolution performance of TNT/hyaAB/PPy in alkaline electrolyte has higher HER performance than that of neutral and acidic electrolytes. These results were consistent with a previous reported study of the pH effect on hydrogenase [59]. To estimate the kinetics of HER, the Tafel slope of TNT/hyaAB/PPy electrode in different pH conditions was measured (Figure 5b). In Tafel plots, the slope of TNT/hyaAB/PPy exhibited following order of pH = 4.5 (461.4 mV dec^{-1}), pH = 7.5 (418.9 mV dec^{-1}), and pH = 10.5 (338.1 mV dec^{-1}). This result denoted that TNT/hyaAB/PPy requires less overpotential for HER due to HER kinetics in alkaline electrolyte than neutral and acidic electrolyte. Furthermore, we conducted ECSA measurement to evaluate the actual electrocatalytic active surface area of the catalyst. The ECSA trend is consistent with the slope of the non-Faradaic current versus scan rate. The cyclic voltammetry (CV) curves were measured at 5–100 mV s^{-1} scan rates in the non-Faradaic region (Figure S4). In ECSA analysis, the slope of TNT/hyaAB/PPy showed the following order of pH = 10.5 (6.80 mF cm^{-2}), pH = 7.5 (6.20 mF cm^{-2}), and pH 4.5 (5.40 mF cm^{-2}) (Figure 5c). This result denotes that the TNT/hyaAB/PPy electrode has more electrocatalytic active sites in alkaline electrolyte for better hydrogen-producing performance than neutral and acidic conditions.

4 | Conclusions

In this study, it was feasible to fabricate the hydrogenase electrode and produce hydrogen by it at an air condition. Hydrogenase 1 of *E. coli* was selected in this study because it has relatively high oxygen tolerance and is easy to be cultivated and extracted. Recombinant plasmid vectors for *E. coli* hydrogenase 1 were made. Hydrogenase expressions were normally operated well by analyzing SDS-PAGE and western blot and in-vitro test for hydrogen production was performed with methylene viologen and sodium dithionite, and manufactured an electropolymerized hydrogenase electrode with purified hydrogenase. It was verified that the electropolymerization with polypyrrole to immobilize *E. coli* hydrogenase on a TNT array has excellent potential for enzyme electrodes in aerobic conditions. It produced 0.224 μmol of H_2 over 2 h in the in-vitro activity test. When hydrogenase was immobilized on a TNT electrode, it showed 205 μA cm^{-2}

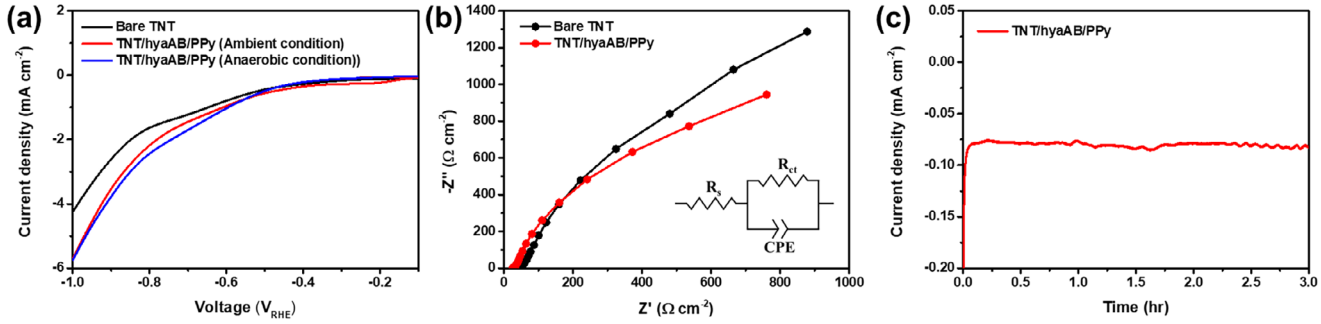

FIGURE 4 | (a) LSV plots of TNT/hyaAB/PPy in aerobic and anaerobic conditions compared to bare TNT, (b) Nyquist plots for charge resistance analysis of TNT depended on TNT/hyaAB/PPy, and (c) chronoamperometry test during 3 h. All tests were conducted in 60 mM MES buffer (pH = 4.5).

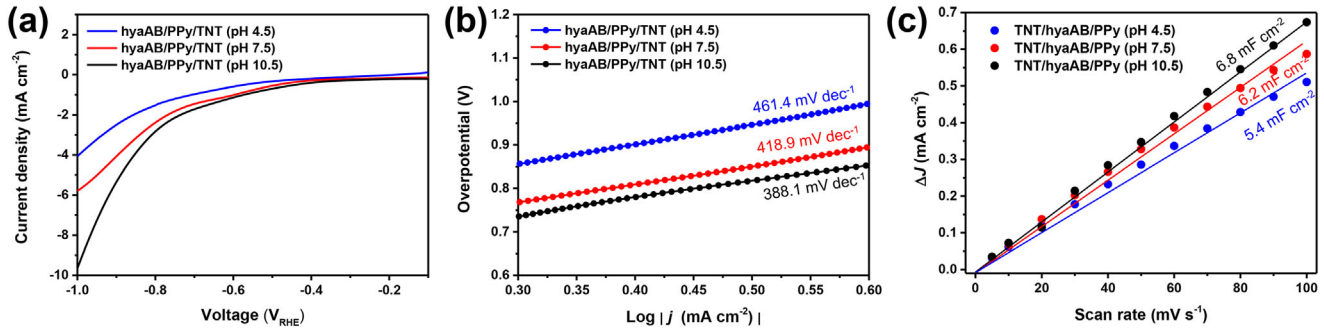

FIGURE 5 | Electrochemical hydrogen evolution performance of the TNT/hyaAB/PPy electrode in different pH of 60 mM MES buffer (pH = 4.5: blue color, pH = 7.5 red color, and pH = 10.5 black color) for (a) LSV plots measured at 5 mV s^{-1} scan rate, (b) Tafel plots measured at 5 mV s^{-1} scan rate, and (c) ECSA analysis measured at 5–100 mV s^{-1}.

current density with applying 0.25 V_{RHE}. Based on the evaluation of the effect on hydrogenase, we confirmed that TNT/hyaAB/PPy exhibits superior HER performance in alkaline electrolyte. Compared with literature data, the TNT/hyaAB/PPy electrode showed relatively high performance, despite the influence of aerobic oxygen for hydrogenase application, as shown in Table S1. Given that [NiFe]-hydrogenase has lower performance and higher oxygen tolerance than [FeFe]-hydrogenase, this value is a relatively good performance. Therefore, we expect that this oxygen-tolerant hydrogenase electrode is one of the potential candidates of BES to produce green hydrogen without CO_2 emission.

Acknowledgments

The authors acknowledge financial support from the Ministry of Science and ICT in Korea (2021R1A2C2009459 and 1.250022).

Conflicts of Interest

The authors declare no conflicts of interest.

Data Availability Statement

The data that support the findings of this study are available from the corresponding author upon reasonable request.

References

1. H. S. Kim, H. Kim, M. C. Flores, G.-S. Jung, and S.-I. In, "Stable Surface Technology for Her Electrodes," *Catalysts* 11, no. 6 (2021): 693, https://doi.org/10.3390/catal11060693.

2. H. C. Lee, H. Kim, and K. Kim, et al., "Unveiling Formation Pathways of Ternary I–III–VI CuInS2 Quantum Dots and Their Effect on Photoelectrochemical Hydrogen Generation," *Advanced Science* 12, no. 31 (2025): e00829, https://doi.org/10.1002/advs.202500829.

3. S. Li, S. Jung, W. Chung, et al., "Defect Engineering of Ternary Cu–In–Se Quantum Dots for Boosting Photoelectrochemical Hydrogen Generation," *Carbon Energy* 5, no. 12 (2023): e384, https://doi.org/10.1002/cey2.384.

4. N. Suresh Powar, S.-I. In, and M. Shanmugam, "Chemically Assembled 2D-van der Waals WSe-WC Heterostructured Photo-anodes for Electrochemical Devices," *FlatChem* 40 (2023): 100523, https://doi.org/10.1016/j.flatc.2023.100523.

5. H. Kim, J. W. Seo, and W. Chung, "Thermal Effect on Photoelectrochemical Water Splitting Toward Highly Solar to Hydrogen Efficiency," *ChemSusChem* 16, no. 11 (2023): e202202017, https://doi.org/10.1002/cssc.202202017.

6. H. Kim, A. Choe, S. B. Ha, et al., "Quantum Dots, Passivation Layer and Cocatalysts for Enhanced Photoelectrochemical Hydrogen Production," *ChemSusChem* 16, no. 3 (2022): e202201925, https://doi.org/10.1002/cssc.202201925.

7. H. R. Kim, G. Kim, S.-I. In, and Y. Park, "Optimization of Porous BiVO 4 Photoanode From Electrodeposited Bi Electrode: Structural Factors Affecting Photoelectrochemical Performance," *Electrochimica Acta* 189 (2016): 252–258, https://doi.org/10.1016/j.electacta.2015.12.106.

8. M. Kim, Y. K. Kim, S. K. Lim, S. Kim, and S.-I. In, "Efficient Visible Light-induced H_2 Production by Au@CdS/TiO_2 Nanofibers: Synergistic Effect of Core–shell Structured Au@CdS and Densely Packed TiO_2 Nanoparticles," *Applied Catalysis B: Environmental* 166–167 (2015): 423–431, https://doi.org/10.1016/j.apcatb.2014.11.036.

9. M. Kim, A. Razzaq, Y. K. Kim, S. Kim, and S.-I. In, "Synthesis and Characterization of Platinum Modified TiO_2-embedded Carbon Nanofibers for Solar Hydrogen Generation," *RSC Advances* 4, no. 93 (2014): 51286–51293, https://doi.org/10.1039/c4ra08455a.

10. K. N. Kim, S. H. Lee, H. Kim, Y. H. Park, and S.-I. In, "Improved Microbial Electrolysis Cell Hydrogen Production by Hybridization With a TiO_2 Nanotube Array Photoanode," *Energies* 11 (2018): 3184, https://doi.org/10.3390/en11113184.

11. S. H. Lee, K.-S. Lee, S. Sorcar, A. Razzaq, C. A. Grimes, and S.-I. In, "Wastewater Treatment and Electricity Generation From a Sunlight-Powered Single Chamber Microbial Fuel Cell," *Journal of Photochemistry and Photobiology A: Chemistry* 358 (2018): 432–440, https://doi.org/10.1016/j.jphotochem.2017.10.030.

12. H.-W. Kim, K.-S. Lee, A. Razzaq, S. H. Lee, C. A. Grimes, and S.-I. In, "Recent Advances in Quantum Dots for Photocatalytic CO_2 Reduction: A Mini-Review," *Energy Technology* 6 (2017): 257, https://doi.org/10.3389/fchem.2021.734108.

13. M. Kim, H. W. Kim, J.-Y. Nam, and S.-I. In, "Recent Progress of Nanostructure Modified Anodes in Microbial Fuel Cells," *Journal of Nanoscience and Nanotechnology* 15 (2015): 6891–6899, https://doi.org/10.1166/jnn.2015.10723.

14. H. R. Pershad, J. L. Duff, H. A. Heering, E. C. Duin, S. P. Albracht, and F. A. Armstrong, "Catalytic Electron Transport in Chromatium Vinosum [NiFe]-Hydrogenase: Application of Voltammetry in Detecting Redox-Active Centers and Establishing That Hydrogen Oxidation Is Very Fast Even at Potentials Close to the Reversible H^+/H^2 Value," *Biochemistry* 38 (1999): 8992–8999, https://doi.org/10.1021/bi990108v.

15. C. Madden, M. D. Vaughn, I. Diez-Perez, et al., "Catalytic Turnover of [FeFe]-Hydrogenase Based on Single-Molecule Imaging," *Journal of the American Chemical Society* 134 (2012): 1577–1582, https://doi.org/10.1021/ja207461t.

16. A. K. Jones, E. Sillery, S. P. Albracht, and F. A. Armstrong, "Direct Comparison of the Electrocatalytic Oxidation of Hydrogen by an Enzyme and a Platinum Catalyst," *Chemical Communications* 8 (2002): 866–867, https://doi.org/10.1039/B201337A.

17. P. M. Vignais, B. Billoud, and J. Meyer, "Classification and Phylogeny of Hydrogenases," *FEMS Microbiology Review* 25 (2001): 455–501, https://doi.org/10.1111/j.1574-6976.2001.tb00587.x.

18. M. Frey, "Hydrogenases: Hydrogen-Activating Enzymes," *ChemBioChem* 3 (2002): 153–160, https://doi.org/10.1002/1439-7633(20020301)3:2/3%3C153::AID-CBIC153%3E3.0.CO;2-B.

19. M. W. W. Adams, "The Structure and Mechanism of Iron-Hydrogenases," *Biochimica et Biophysica Acta* 1020 (1990): 115–145, https://doi.org/10.1016/0005-2728(90)90044-5.

20. B. Bleijlevens, T. Buhrke, E. van der Linden, B. Friedrich, and S. P. J. Albracht, "The Auxiliary Protein HypX Provides Oxygen Tolerance to the Soluble [NiFe]-Hydrogenase of Ralstonia Eutropha H16 by Way of a Cyanide Ligand to Nickel," *Journal of Biological Chemistry* 279 (2004): 46686–46691, https://doi.org/10.1074/jbc.M406942200.

21. A. Volbeda, C. Darnault, A. Parkin, F. Sargent, F. A. Armstrong, and J. C. Fontecilla-Camps, "Crystal Structure of the O_2-Tolerant Membrane-Bound Hydrogenase 1 From *Escherichia coli* in Complex With Its Cognate Cytochrome b," *Structure (London, England)* 21 (2013): 184–190, https://doi.org/10.1016/j.str.2012.11.010.

22. D. Evvyernie, K. Morimoto, S. Karita, T. Kimura, K. Sakka, and K. Ohmiya, "Conversion of Chitinous Wastes to Hydrogen Gas by *Clostridium paraputrificum* M-21," *Journal of Bioscience and Bioengineering* 91 (2001): 339–343, https://doi.org/10.1016/S1389-1723(01)80148-1.

23. C. Y. Lin and C. H. Lay, "Carbon/Nitrogen-Ratio Effect on Fermentative Hydrogen Production by Mixed Microflora," *International Journal of Hydrogen Energy* 29 (2004): 41–45, https://doi.org/10.1016/S0360-3199(03)00083-1.

24. C. C. Wang, C. W. Chang, C. P. Chu, D. J. Lee, B.-V. Chang, and C. S. Liao, "Producing Hydrogen From Wastewater Sludge by *Clostridium bifermentans*," *Journal of Biotechnology* 102 (2003): 83–92, https://doi.org/10.1016/s0168-1656(03)00007-5.

25. H. Yokoi, A. Saitsu, H. Uchida, J. Hirose, S. Hayashi, and Y. Takasaki, "Microbial Hydrogen Production From Sweet Potato Starch Residue," *Journal of Bioscience and Bioengineering* 91 (2001): 58–63, https://doi.org/10.1016/S1389-1723(01)80112-2.

26. H.-S. Shin, J.-H. Youn, and S.-H. Kim, "Hydrogen Production From Food Waste in Anaerobic Mesophilic and Thermophilic Acidogenesis," *International Journal of Hydrogen Energy* 29 (2004): 1355–1363, https://doi.org/10.1016/j.ijhydene.2003.09.011.

27. T. Kanai, H. Imanaka, A. Nakajima, et al., "Continuous Hydrogen Production by the Hyperthermophilic Archaeon, *Thermococcus kodakaraensis* KOD1," *Journal of Biotechnology* 116 (2005): 271–282, https://doi.org/10.1016/j.jbiotec.2004.11.002.

28. S.-H. Kim, S.-K. Han, and H.-S. Shin, "Feasibility of Biohydrogen Production by Anaerobic Co-digestion of Food Waste and Sewage Sludge," *International Journal of Hydrogen Energy* 29 (2004): 1607–1616, https://doi.org/10.1016/j.ijhydene.2004.02.018.

29. D. H. Nam, J. Z. Zhang, V. Andrei, et al., "Solar Water Splitting With a Hydrogenase Integrated in Photoelectrochemical Tandem Cells," *Angewandte Chemie International Edition* 57 (2018): 10595–10599, https://doi.org/10.1002/anie.201805027.

30. R. A. Rozendal, A. W. Jeremiasse, H. V. Hamelers, and C. J. Buisman, "Hydrogen Production With a Microbial Biocathode," *Environmental Science & Technology* 42 (2007): 629–634, https://doi.org/10.1021/es071720.

31. Y. Zhao, N. C. Anderson, M. W. Ratzloff, et al., "Proton Reduction Using a Hydrogenase-Modified Nanoporous Black Silicon Photoelectrode," *ACS Applied Materials & Interfaces* 8 (2016): 14481–14487, https://doi.org/10.1021/acsami.6b00189.

32. S. Bae, E. Shim, J. Yoon, et al., "Photoanodic and Cathodic Role of Anodized Tubular Titania in Light-Sensitized Enzymatic Hydrogen Production," *Journal of Power Sources* 185 (2008): 439–444, https://doi.org/10.1016/j.jpowsour.2008.06.094.

33. Y. Asada and J. Miyake, "Photobiological Hydrogen Production," *Journal of Bioscience and Bioengineering* 88 (1999): 1–6, https://doi.org/10.1016/S1389-1723(99)80166-2.

34. A. A. Tsygankov, A. S. Fedorov, S. N. Kosourov, and K. K. Rao, "Hydrogen Production by Cyanobacteria in an Automated Outdoor Photobioreactor Under Aerobic Conditions," *Biotechnology and Bioengineering* 80 (2002): 777–783, https://doi.org/10.1002/bit.10431.

35. A. A. Tsygankov, L. T. Serebryakova, K. K. Rao, and D. O. Hall, "Acetylene Reduction and Hydrogen Photoproduction by Wild-Type and Mutant Strains of Anabaena at Different CO_2 and O_2 Concentrations," *FEMS Microbiology Letters* 167 (1998): 13–17, https://doi.org/10.1111/j.1574-6968.1998.tb13201.x.

36. V. Shah, N. Garg, and D. Madamwar, "Ultrastructure of the Fresh Water Cyanobacterium Anabaena Variabilis SPU 003 and Its Application for Oxygen-Free Hydrogen Production," *FEMS Microbiology Letters* 194 (2001): 71–75, https://doi.org/10.1111/j.1574-6968.2001.tb09448.x.

37. S. V. Morozov, P. M. Vignais, L. Cournac, et al., "Bioelectrocatalytic Hydrogen Production by Hydrogenase Electrodes," *International Journal of Hydrogen Energy* 27 (2002): 1501–1505, https://doi.org/10.1016/S0360-3199(02)00091-5.

38. K. P. Sokol, W. E. Robinson, J. Warnan, et al., "Bias-Free Photoelectrochemical Water Splitting With Photosystem II on a Dye-Sensitized Photoanode Wired to Hydrogenase," *Nature Energy* 3 (2018): 944–951, https://doi.org/10.1038/s41560-018-0232-y.

39. B. H. Jo and H. J. Cha, "Activation of Formate Hydrogen-Lyase via Expression of Uptake [NiFe]-Hydrogenase in *Escherichia coli* BL21(DE3)," *Microbial Cell Factories* 14 (2015): 151, https://doi.org/10.1186/s12934-015-0343-0.

40. A. Yoshida, T. Nishimura, H. Kawaguchi, M. Inui, and H. Yukawa, "Enhanced Hydrogen Production From Formic Acid by Formate Hydrogen Lyase-Overexpressing *Escherichia coli* Strains," *Applied and Environmental Microbiology* 71 (2005): 6762–6768, https://doi.org/10.1128/AEM.71.11.6762-6768.2005.

41. T. Maeda, V. Sanchez-Torres, and T. K. Wood, "Enhanced Hydrogen Production From Glucose by Metabolically Engineered *Escherichia coli*," *Applied Microbiology and Biotechnology* 77 (2007): 879–890, https://doi.org/10.1007/s00253-007-1217-0.

42. T. Maeda, V. Sanchez-Torres, and T. K. Wood, "Metabolic Engineering to Enhance Bacterial Hydrogen Production," *Microbial Biotechnology* 1 (2007): 30–39, https://doi.org/10.1111/j.1751-7915.2007.00003.x.

43. G. Vardar-Schara, T. Maeda, and T. K. Wood, "Metabolically Engineered Bacteria for Producing Hydrogen via Fermentation," *Microbial Biotechnology* 1 (2007): 107–125, https://doi.org/10.1111/j.1751-7915.2007.00009.x.

44. K. Francis, P. Patel, J. C. Wendt, and K. T. Shanmugam, "Purification and Characterization of Two Forms of Hydrogenase Isoenzyme 1 From *Escherichia coli*," *Journal of Bacteriology* 172 (1990): 5750–5757, https://doi.org/10.1128/jb.172.10.5750-5757.1990.

45. A. Melis, "Green Alga Hydrogen Production: Progress, Challenges and 3 Prospects," *International Journal of Hydrogen Energy* 27 (2002): 1217–1228, https://doi.org/10.1016/S0360-3199(02)00110-6.

46. M. L. Ghirardi, L. Zhang, J. W. Lee, et al., "Microalgae: A Green Source of Renewable H_2," *Trends in Biotechnology* 18 (2000): 506–511, https://doi.org/10.1016/S0167-7799(00)01511-0.

47. J. Y. H. Kim, B. H. Jo, and H. J. Cha, "Production of Biohydrogen by Recombinant Expression of [NiFe]-Hydrogenase 1 in *Escherichia coli*," *Microbial Cell Factories* 9 (2010): 54, https://doi.org/10.1186/1475-2859-9-54.

48. T. Maeda, V. Sanchez-Torres, and T. K. Wood, "Protein Engineering of Hydrogenase 3 to Enhance Hydrogen Production," *Applied Microbiology and Biotechnology* 79 (2008): 77–86, https://doi.org/10.1007/s00253-008-1416-3.

49. H. Krassen, A. Schwarze, B. Friedrich, K. Ataka, O. Lenz, and J. Heberle, "Photosynthetic Hydrogen Production by a Hybrid Complex of Photosystem I and [NiFe]-hydrogenase," *ACS Nano* 3 (2009): 4055–4061, https://doi.org/10.1021/nn900748j.

50. J. Yoon, S. Bae, E. Shim, and H. Joo, "Pyrococcus Furiosus-Immobilized Anodized Tubular Titania Cathode in a Hydrogen Production System," *Journal of Power Sources* 189 (2009): 1296–1301, https://doi.org/10.1016/j.jpowsour.2008.12.072.

51. K. A. Brown, S. Dayal, X. Ai, G. Rumbles, and P. W. King, "Controlled Assembly of Hydrogenase-CdTe Nanocrystal Hybrids for Solar Hydrogen Production," *Journal of the American Chemical Society* 132 (2010): 9672–9680, https://doi.org/10.1021/ja101031r.

52. M. Hambourger, M. Gervaldo, D. Svedruzic, et al., "[FeFe]-Hydrogenase-Catalyzed H2 Production in a Photoelectrochemical Biofuel Cell," *Journal of the American Chemical Society* 130 (2008): 2015–2022, https://doi.org/10.1021/ja077691k.

53. M. L. Helm, M. P. Stewart, R. M. Bullock, M. R. DuBois, and D. L. DuBois, "A Synthetic Nickel Electrocatalyst With a Turnover Frequency Above 100,000 s^{-1} for H_2 Production," *Science* 333 (2001): 863–866, https://doi.org/10.1126/science.1205864.

54. N. Kosem, M. Watanabe, J. T. Song, A. Takagaki, and T. Ishihara, "A Comprehensive Study on Rational Biocatalysts and Individual Components of Photobiocatalytic H_2 Production Systems," *Applied Catalysis A: General* 651 (2023): 119019, https://doi.org/10.1016/j.apcata.2022.119019.

55. H. D. Peck and H. Gest, "A New Procedure for Assay of Bacterial Hydrogenases," *Journal of Bacteriology* 71 (1956): 70–80, https://doi.org/10.1128/jb.71.1.70-80.1956.

56. N. Tamiya, Y. Kondo, T. Kameyama, and S. Akabori, "Determination of Hydrogenase by the Hydrogen Evolution From Reduced Methylviologen," *Journal of Biochemistry* 42 (1955): 613–614, https://doi.org/10.1093/oxfordjournals.jbchem.a126566.

57. S. V. Makarov, E. V. Kudrik, R. van Eldik, and E. V. Naidenko, "Reactions of Methyl Viologen and Nitrite With Thiourea Dioxide. New Opportunities for an Old Reductant," *Journal of the Chemical Society, Dalton Transactions* 22 (2002): 4074–4076, https://doi.org/10.1039/B209195J.

58. P.-H. Zhao, B. Jin, S.-J. Wang, D. Wang, Y. Guo, and T.-P. Hu, "Variation of Dithiolate Bridges in Carbon Nanotube-Attached Diiron Chelate Compounds for Electrocatalytic Hydrogen Evolution Reaction," *Applied Surface Science* 639 (2023): 158276, https://doi.org/10.1016/j.apsusc.2023.158276.

59. S.-J. Wang, Y. Gao, X. Su, Y.-Z. Wang, Y.-P. Qu, and P.-H. Zhao, "Aqueous pH Influence on the Electrocatalytic Hydrogen Evolution Reaction With Carbon Nanotube-Supported Diiron Dithiolato Compound," *Applied Surface Science* 661 (2024): 160074, https://doi.org/10.1016/j.apsusc.2024.160074.

Supporting Information

Additional supporting information can be found online in the Supporting Information section.

Supplementary file 1: nano70069-sup-0001-SuppMat.docx